



LAWRENCE  
LIVERMORE  
NATIONAL  
LABORATORY

LLNL-TR-799197

# 2019 LLNL Nuclear Science and Security Summer Internship Program

M. Zavarin

December 11, 2019

## **Disclaimer**

---

This document was prepared as an account of work sponsored by an agency of the United States government. Neither the United States government nor Lawrence Livermore National Security, LLC, nor any of their employees makes any warranty, expressed or implied, or assumes any legal liability or responsibility for the accuracy, completeness, or usefulness of any information, apparatus, product, or process disclosed, or represents that its use would not infringe privately owned rights. Reference herein to any specific commercial product, process, or service by trade name, trademark, manufacturer, or otherwise does not necessarily constitute or imply its endorsement, recommendation, or favoring by the United States government or Lawrence Livermore National Security, LLC. The views and opinions of authors expressed herein do not necessarily state or reflect those of the United States government or Lawrence Livermore National Security, LLC, and shall not be used for advertising or product endorsement purposes.

This work performed under the auspices of the U.S. Department of Energy by Lawrence Livermore National Laboratory under Contract DE-AC52-07NA27344.



# 2019 LLNL Nuclear Science and Security Summer Internship Program



Glenn T. Seaborg Institute  
Lawrence Livermore National Laboratory  
Physical and Life Sciences Directorate  
Livermore, CA 94550

Director: Mavrik Zavarin ([zavarin1@llnl.gov](mailto:zavarin1@llnl.gov))  
Administrator: Keisha Hamilton  
Website: <https://seaborg.llnl.gov/>



Sponsors:  
Defense Threat Reduction Agency, Department of Defense  
Glenn T. Seaborg Institute, Physical and Life Sciences Directorate, Lawrence Livermore National Laboratory



Lawrence Livermore National Laboratory is operated by Lawrence Livermore National Security, LLC, for the U.S. Department of Energy, National Nuclear Security Administration under Contract DE-AC52-07NA27344.  
LLNL-TR-799197

## **Disclaimer**

This document was prepared as an account of work sponsored by an agency of the United States government. Neither the United States government nor Lawrence Livermore National Security, LLC, nor any of their employees makes any warranty, expressed or implied, or assumes any legal liability or responsibility for the accuracy, completeness, or usefulness of any information, apparatus, product, or process disclosed, or represents that its use would not infringe privately owned rights. Reference herein to any specific commercial product, process, or service by trade name, trademark, manufacturer, or otherwise does not necessarily constitute or imply its endorsement, recommendation, or favoring by the United States government or Lawrence Livermore National Security, LLC. The views and opinions of authors expressed herein do not necessarily state or reflect those of the United States government or Lawrence Livermore National Security, LLC, and shall not be used for advertising or product endorsement purposes.

## **Auspices**

This work was performed under the auspices of the U.S. Department of Energy by Lawrence Livermore National Laboratory under Contract DE-AC52-07NA273.

## 2019 Nuclear Science and Security Summer Internship Program



**2019 Nuclear Science and Security Summer Internship Program** students met with DTRA management on August 7, 2019. From left: **Silvina DiPietro** (Florida International University), **Orlando Gomez** (Notre Dame University, DTRA intern), **Michael Klosterman** (University of Utah, DTRA intern), **Catherine Apgar** (UC Berkeley, DTRA intern), **Meena Said** (University of Notre Dame, DTRA/Safeguards intern), **Frances Zengotita** (Florida International University), **Jill Rahon** (West Point), **Jacob Lewis** (UC Riverside, DTRA intern), **Jacqueline Garcia** (Oregon State University, DTRA intern), **Amalie Zeitoun** (DTRA acting chief of staff), **Damon Anderson** (UC Berkeley, DTRA intern), **Thomas Early** (DTRA Human Resources), and **Mavrik Zavarin** (LLNL Seaborg Institute director).

The Lawrence Livermore National Laboratory (LLNL) Nuclear Science and Security Summer Internship Program (NS<sup>3</sup>IP) is designed to give graduate students an opportunity to come to LLNL for 8–10 weeks of hands-on research. Students conduct research under the supervision of a staff scientist, attend a weekly lecture series, interact with other students, and present their work in poster format at the end of the program. Students also have the opportunity to meet staff scientists one-on-one, participate in LLNL facility tours (e.g., the National Ignition Facility and Center for Accelerator Mass Spectrometry), and gain a better understanding of the various science programs at LLNL.

Currently titled the Nuclear Science and Security Summer Internship Program, this program began over 20 years ago as the Actinide Sciences Summer Program. The program is run by the Glenn T. Seaborg Institute in the Physical and Life Sciences Directorate at LLNL. The goal of the NS<sup>3</sup>IP is to facilitate the training of next generation nuclear scientists and engineers to solve critical national security problems in the field of nuclear science and nuclear security. Students are selected from the fields of physics, chemistry, geology, mathematics, nuclear engineering, chemical engineering and environmental sciences. Students engage in research projects in the disciplines of actinide chemistry, radiochemistry, isotopic analysis, computation, radiation detection, and nuclear engineering. This Internship Program is supported by the Defense Threat Reduction Agency (DTRA) which enables the Department of Defense and the U.S. Government to prepare for and combat weapons of mass destruction and

improvised threats and to ensure nuclear deterrence. The internship program is intended to strengthen the “pipeline” for future scientific disciplines critical to DTRA and DOE.

The NS<sup>3</sup>IP is highly competitive, with over 250 applications received in 2019 for the 7-8 available slots. Additional students funded through paid internships and fellowships from NNSA and DOE are invited to participate in the summer lecture series and poster symposium. This year, the NS<sup>3</sup>IP hosted students from 6 universities (see Table 1) across the United States (Figure 1). The NS<sup>3</sup>IP students conducted research on such diverse topics as field portable and laboratory radiation detector development, pre- and post-detonation mass spectrometry, nuclear signatures development, and fundamental nuclear physics (see Table 2 for poster titles). Continued research collaboration between the graduate student, faculty advisor, and LLNL mentors is strongly encouraged. In many cases, NS<sup>3</sup>IP research evolves into a significant component of the students’ graduate theses. For example, two graduates of the 2019 NS<sup>3</sup>IP (Damon Anderson and Orlando Gomez) are continuing their collaboration with LLNL staff and incorporating their summer projects into their PhD research.

In addition to hands-on training, students attend a weekly lecture series on topics applicable to the field of nuclear science (Table 3). Speakers are selected to represent the breadth of expertise that is required for nuclear science research. Speakers discuss the importance of their work in the context of national and international nuclear security efforts.

Graduate and undergraduate students on fellowships such as the DOE Environmental Management traineeship program and Nuclear Safeguards internship program, are invited to join our summer internship activities. This year, LLNL hosted 4 students from Washington State University and Florida International University through nuclear science fellowships and programmatic funding.

Our summer program is providing a nuclear science pipeline of top-quality students from universities across the United States. Since 2002, 30-40% have returned to conduct their graduate research at LLNL. In addition:

- 32 interns continued their graduate work at LLNL (9 of which received fellowships)
- 18 became postdoctoral fellows at LLNL
- 7 became postdoctoral fellows at other national labs
- 13 were hired as career scientists at LLNL
- 5 were hired as career scientists at other national labs
- 4 were hired as faculty in the area of nuclear forensics/radiochemistry/nuclear science
- 4 were hired at other government institutions

A big factor in the success of this program is the dedication of the staff scientists (predominantly DTRA funded) who volunteer to mentor the summer students. Four of our 2019 mentors are, in fact, alumni of the Seaborg Institute summer internship programs. The mentors develop summer projects for their students, oversee necessary safety training, and dedicate time to helping the interns and students maximize their productivity and scientific potential. This internship program would not be possible without the mentors’ dedication. Posters summarizing the 2019 NS<sup>3</sup>IP student research were presented at our Laboratory Student Poster Day and are included at the end of this report.

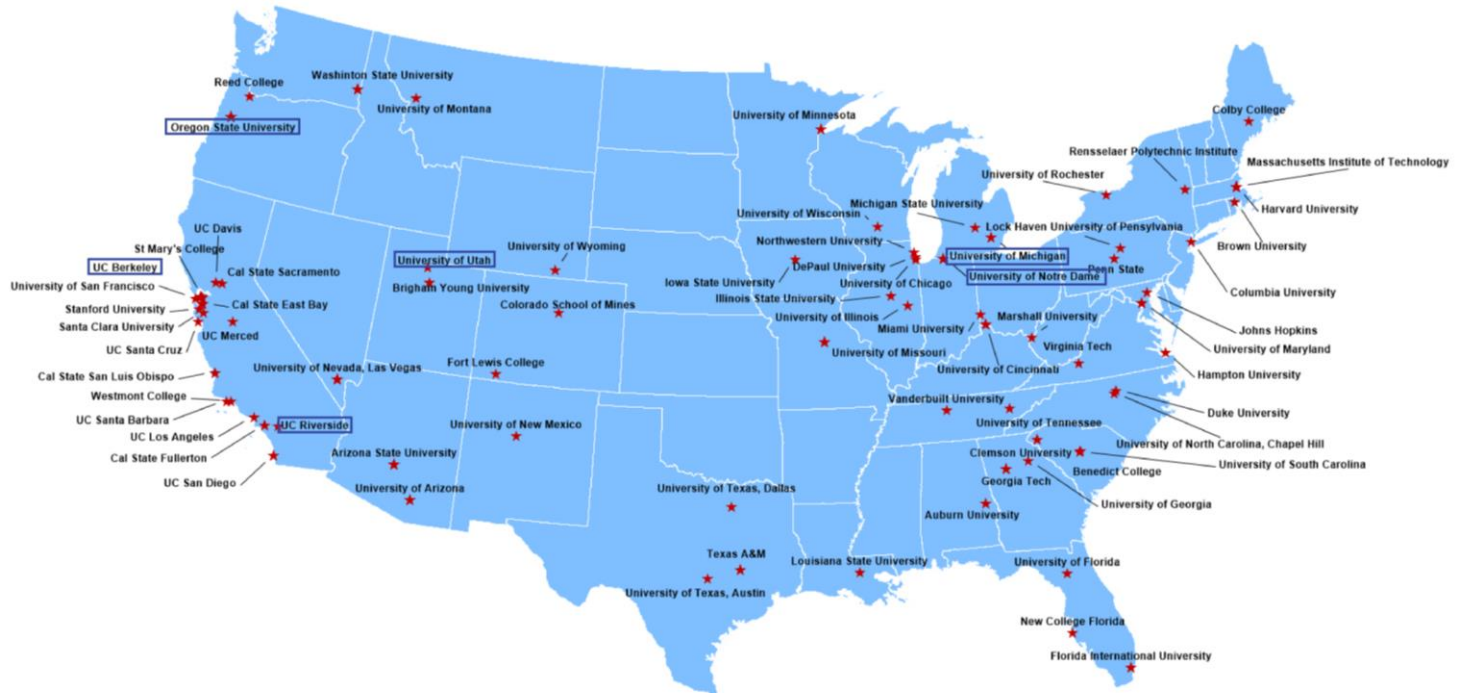


**Figure 1.** The Seaborg Institute summer interns come from universities from across the United States. Universities associated with the 2019 Nuclear Science and Security Summer Internship program are highlighted with a blue outline.

**Table 1. 2019 Nuclear Science and Security Summer Internship Program Students**

Student	Major	University	Year
Damon Anderson	Nuclear Engineering	UC Berkeley	Undergraduate <sup>1</sup>
Orlando Gomez	Physics	University of Notre Dame	Graduate
Michael Klosterman	Nuclear Engineering	University of Utah	Graduate
Lauren Finney/Ibon	Chemistry	University of Michigan	Graduate
Catherine Apgar	Nuclear Engineering	UC Berkeley	Graduate
Jaqueline Garcia	Health Physics	Oregon State University	Graduate
Jacob Lewis	Materials Science	UC Riverside	Graduate
Meena Said <sup>2</sup>	Nuclear Engineering	University of Notre Dame	Graduate

<sup>1</sup> Accepted to graduate school at the University of Michigan.

<sup>2</sup> Partially supported by the Nuclear Safeguards program.

**Table 2. 2019 Nuclear Science and Security Summer Internship Program Student Projects and Mentors**

Student	Mentor	Project Poster Title
Damon Anderson	Nerine Cherepy	ASIC Development and Testing For a DTRA-Funded Circuit
Orlando Gomez	Jutta Escher	Refining Nuclear Mass Models using Bayesian Neural Networks
Michael Klosterman	Mike Singleton	Fractionation of Oxygen Isotopes in Uranium Oxides
Lauren Finney/Ibon	David Weisz	Infrared Absorption Spectroscopy to Study Oxide Formation in Laser Produced Plasmas for Nuclear Forensics Applications
Catherine Apgar	Pihong Zhao and Kevin Roberts	Quantifying Uncertainty in Inter-Laboratory Thermal Calibration Exercise
Jaqueline Garcia	Tashi Parsons-Davis	Gamma-Gamma Coincidence Counting for Radioisotope Detection
Jacob Lewis	Brett Isselhardt and Mike Savina	Resonance Ionization Mass Spectrometry applications
Meena Said	Naomi Marks	Measuring Surface Roughness on UO <sub>2</sub> Fuel Pellets for Nuclear Forensics

**Table 3. 2019 Nuclear Science and Security Summer Internship Program Seminar Schedule**

Date	Speaker	Topic
6/19/19	<b>Jutta Escher</b> <i>Staff Scientist, Nuclear Data &amp; Theory Nuclear and Chemical Sciences Division</i>	Nuclear Reaction Research for Astrophysics and Lab Applications
6/26/19	<b>Nerine Cherepy</b> <i>Staff Scientist Materials Sciences Division</i>	New Scintillators and their Integration into Detector Systems
7/3/19	<b>Mike Savina</b> <i>Staff Scientist, Chemical &amp; Isotopic Signatures Nuclear and Chemical Sciences Division</i>	Starry Messengers: Stardust Grains Deliver Stellar News to Earth
7/10/19	<b>David Weisz</b> <i>Staff Scientist, Chemical &amp; Isotopic Signatures Nuclear and Chemical Sciences Division</i>	Laser-based spectroscopy to inform post-detonation chemistry
7/19/19	<b>Naomi Marks</b> <i>Staff Scientist, Chemical &amp; Isotopic Signatures Nuclear and Chemical Sciences Division</i> <b>SAN JOSE ACS SUMMER STUDENT VISIT</b>	Nuclear Forensics Materials Signatures at the front end of the Fuel Cycle
7/24/19	<b>Ruth Kips</b> <i>Staff Scientist, Chemical &amp; Isotopic Signatures Nuclear and Chemical Sciences Division</i>	LLNL's International Nuclear Forensics Program
7/31/19	<b>Ping Yang</b> <i>Los Alamos National Laboratory</i>	Predictive Modeling of Actinide Chemistry
8/9/19	<b>Mavrik Zavarin</b> <i>Director, Glenn T. Seaborg Institute Physical and Life Sciences Directorate</i>	Close Out

**DTRA Agenda**

PHYSICAL AND LIFE SCIENCES DIRECTORATE  
GLENN T. SEABORG INSTITUTE

**AMALIE ZEITOUN, THOMAS EARLY, JILL RAHON**

Defense Threat Reduction Agency

**AUGUST 7, 2019**

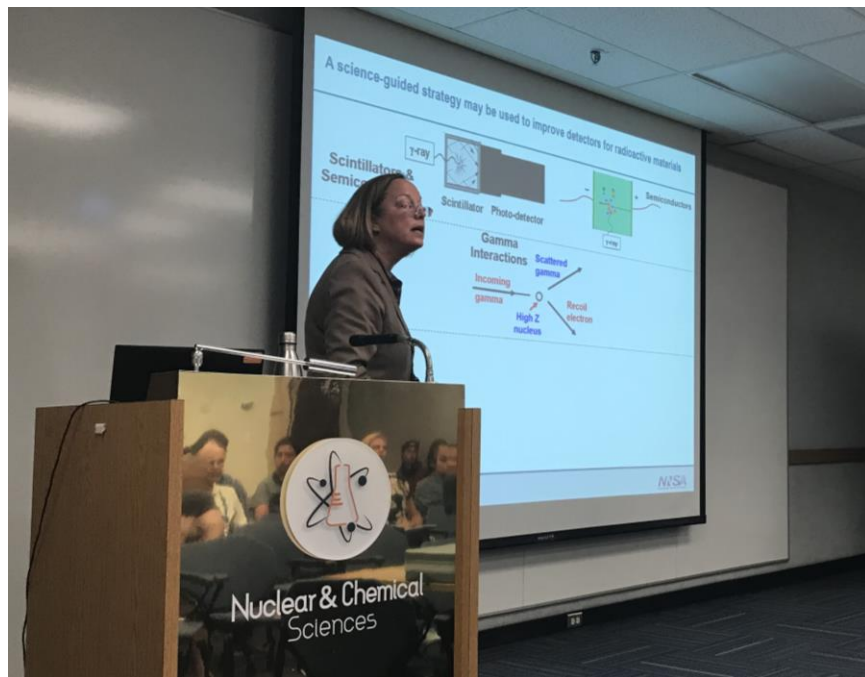
9:45 A.M.	Arrival at West Gate Badge Office	Met by Mavrik Zavarin
10:00 A.M.	Introductions DTRA Summer Interns and Mentors	B151 R1101 Ouija room
11:00 A.M.	SEMINAR Thomas Early, DTRA Mission Overview	B154 R1013 OUO – No Foreign Nationals
12:00 P.M.	LUNCH Mavrik Zavarin	Central Cafe
1:15 P.M.	Lab Tours David Weisz	B151 Lab Tour of Counting Facility (Thomas), Laser Plasma Lab (Weisz), RIMS (Savina)
2:30 P.M.	Student Poster Session David Weisz, Naomi Marks	B543 Atrium
4:00 P.M*	Depart*	

\* B151 Ouija room will be reserved until 5pm for followon discussions if needed.

## **2019 NS<sup>3</sup>IP in Pictures**



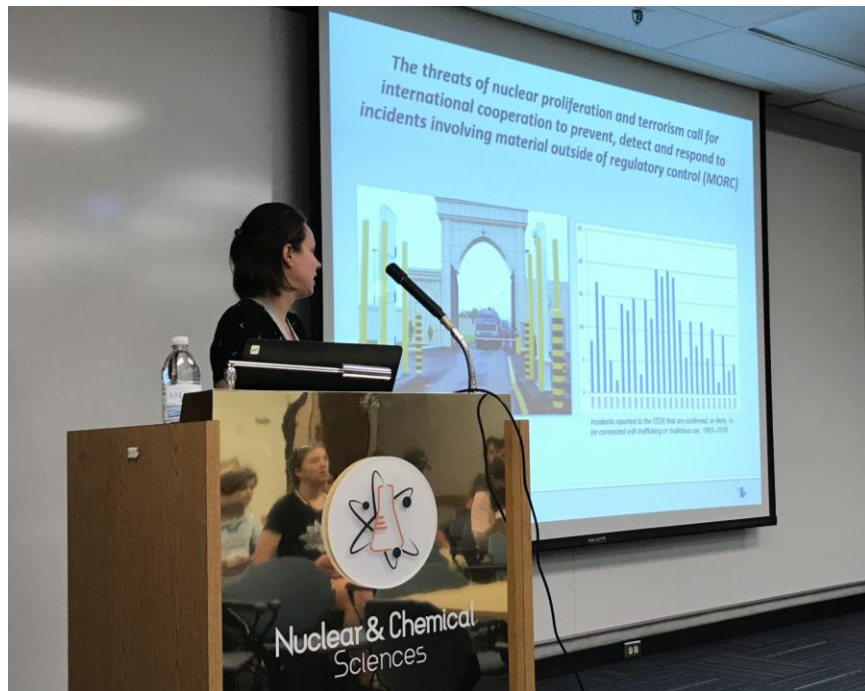
**Dr. Jutta Escher describes the role of nuclear theory in nuclear science and security.**



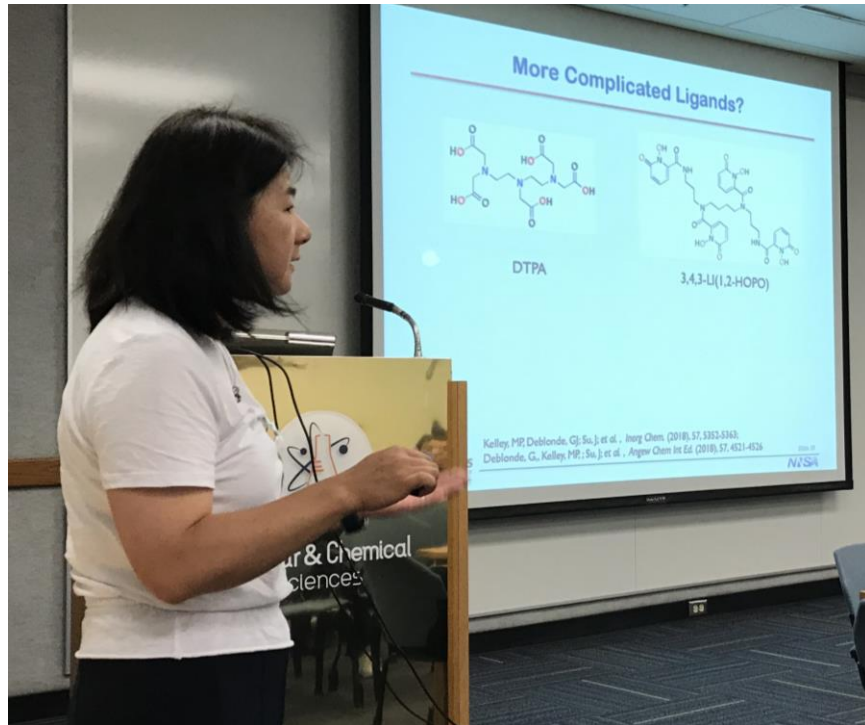
**Dr. Nerine Cherepy describing the fundamentals of radiation detection.**



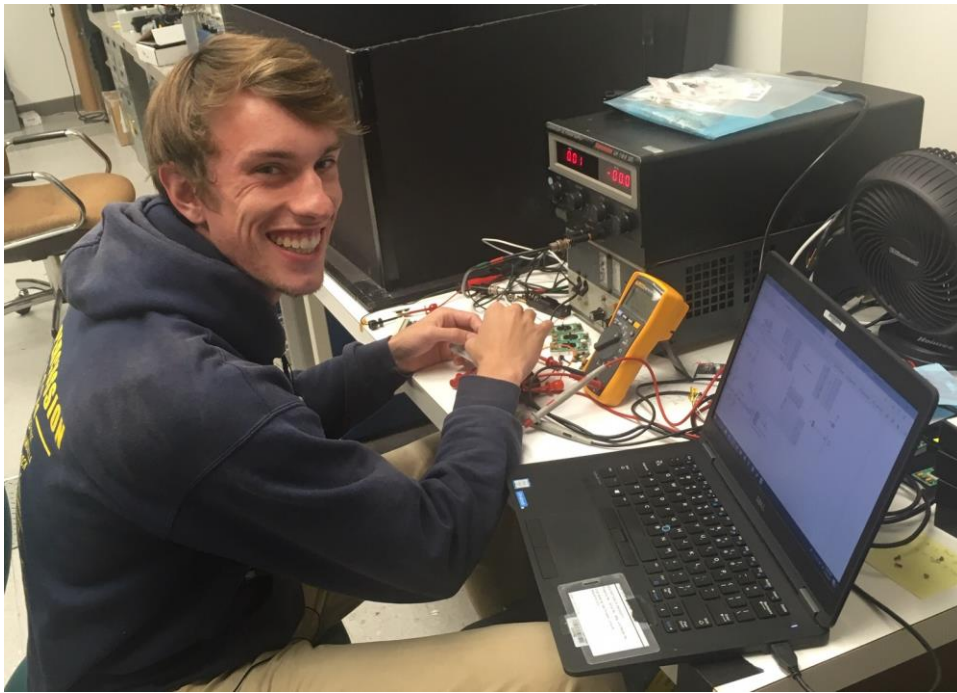
**Dr. David Weisz describes the processes controlling formation of nuclear fallout.**



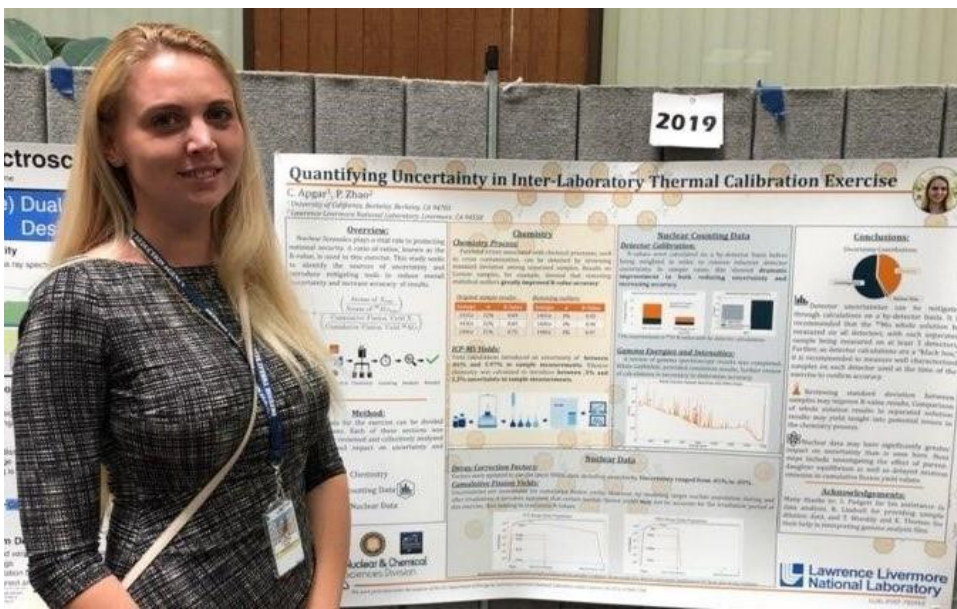
**Dr. Ruth Kips presents an overview of international nuclear nonproliferation.**



**Dr. Ping Yang describes the fundamental chemistry of actinides.**



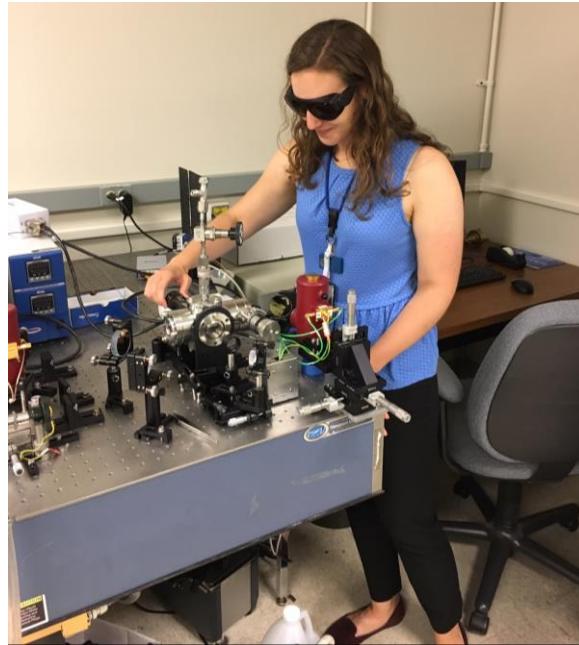
**Damon Anderson works on radiation detection circuits.**



**Catherine Apgar presents research in uncertainty quantification at the poster symposium.**



**Michael Klosterman works on uranium oxide fluorination and oxygen isotope separation.**



**Lauren Ibon works on laser spectroscopy under simulated nuclear detonation conditions.**

**2019 NS<sup>3</sup>IP Student Posters**



LLNL-POST-784318

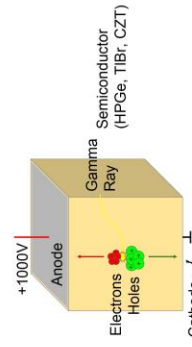
# High Resolution Gamma Ray Spectroscopy

Damon Anderson, Sean O'Neal, Erik Swanberg, Nerine Cherepy, Steve Payne

## Multisource Energy Characterization of Thallium Bromide

### Semiconductor Radiation Detectors

A gamma ray interacts with a biased semiconductor creating charge carriers that subsequently create signals on electrodes.



### Pixelated Thallium Bromide

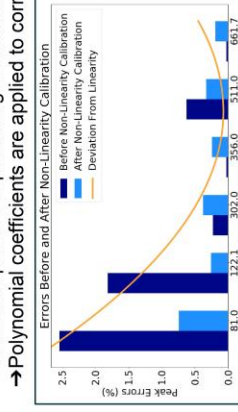
→ Thallium Bromide:  
◆ High Z: (Tl, 81) and (Br, 35)  
◆ High Band Gap: 2.6 eV

→ Pixelation:  
◆ Single polarity charge sensing  
◆ 3D spatial resolution

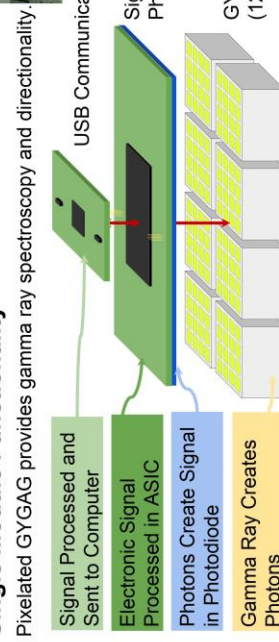


### Non-Linearity Characterization

→ Spectra taken for  $^{22}\text{Na}$ ,  $^{57}\text{Co}$ ,  $^{133}\text{Ba}$ , and  $^{137}\text{Cs}$   
→ Measured peaks are plotted against the known peaks to determine linearity  
→ Polynomial coefficients are applied to correct peak errors



### Single Module Functionality



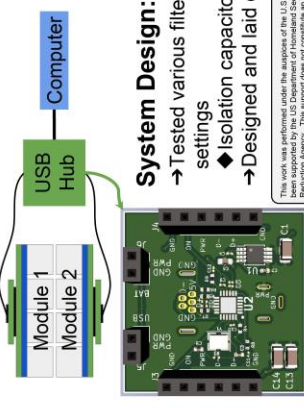
### Dual Module Considerations:

→ Electronic Noise:  
◆ Module cross-talk destroys signal

◆ Solution: Aluminum shielding mitigates module cross-talk

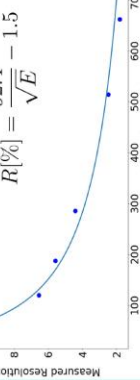
→ Temperature:  
◆ On-board linear regulators dissipate heat due to overdriving the voltage

◆ Solution: In module cooling is required



### Resolution Characterization

→ Resolution tails off as energy increases as expected  
→ Negative offset implies systematic error in measurement  
◆ Limiting energy resolution ( $E = \infty$ ) must be positive



→ Tested various filtering configurations and shielding/temperature settings  
◆ Isolation capacitors, power line inductors, grounding connections  
→ Designed and laid out PCB implementing the desired configuration

This work was performed under the auspices of the U.S. Department of Energy by Lawrence Livermore National Laboratory under Contract DE-AC52-07NA24394 and has been performed under the auspices of the U.S. Department of Homeland Security, Countermeasures Division of Mass Detection Office. We also appreciate the support from the Defense Threat Reduction Agency.

This support does not constitute an expressed or implied endorsement on the part of the Government.

LLNL-POST-



# Refining Nuclear Mass Models using Bayesian Neural Networks

  
O.Olivas-Gomez<sup>1</sup>, K.D.Humbird<sup>2</sup>, J.E.Escher<sup>2</sup>, M.G.Kruse<sup>2</sup>  
University of Notre Dame, Notre Dame, IN 46556  
<sup>2</sup>Lawrence Livermore National Laboratory, 7000 East Ave, Livermore CA 94550

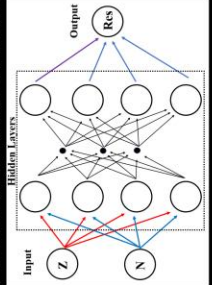
## Introduction

Constraining nuclear masses far from stability is of paramount importance in Nuclear Physics. Nuclear masses for stability help us better understand nucleosynthesis in hot stellar environments (e.g. novae) as well as understanding the causal composition of cold neutron stars. Even with recent advances in experimental techniques and facilities, many of these nuclei remain beyond experimental reach. Therefore we rely on theoretical mass models and their extrapolations to make predictions about neutron-rich isotopes far from stability. However, many nuclear mass models disagree dramatically once extrapolated [4] (see fig. 1).

In recent studies, Bayesian Neural Networks (BNN), a machine learning tool, have been shown to improve nuclear mass model predictions as well as estimate their uncertainties [1]. Using DJINN, a decision tree to neural network mapping algorithm (see next panel), we develop our own refined nuclear mass models. We compare our models with those in the literature, as well as make predictions of the limit of nuclear stability, the neutron drip-line.

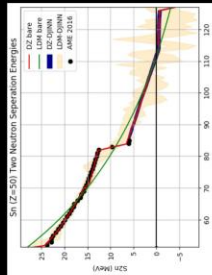
## Neural Networks & DJINN:

Neural networks trained via supervised learning can discover subtle relationships between variables and are well-suited for complex physical systems. However, it is difficult to design and train an accurate model. Deep Jointly-Informed Neural Networks (DJINN) combines the user-friendly features of tree-based models with the accuracy, flexibility, and scalability of deep neural networks [3]. The algorithm first models the data using decision trees and then produces a network with hidden layers, neurons, and initial weights that reflect the decision tree structure. The neural network is subsequently trained using back-propagation to optimize predictive performance. The inclusion of drop-out layers work as a Bayesian Approximation allowing statistical estimates of the uncertainties in the model predictions [5].

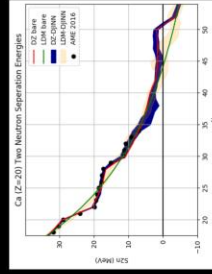


## Results:

With nuclear masses, one application is to calculate neutron separation energies.  $S_{2n}(Z, N) = M(Z, N) - M(Z, N-1)$  and  $S_{1n}(Z, N) = M(Z, N) - M(Z, N-2)$ . Of particular interest is when  $S_{2n} < 0$  and the nucleus becomes unstable to neutron emission.



According to DJ-DJINN model,  $^{108}\text{Sn}$  is not particle stable ( $N = 120$  magic number).



The DJ-DJINN model predicts that  $^{76}\text{Ca}$  is the last stable isotope along the  $Z=20$  chain.

## Discussion / Future Work

Using DJINN, we can refine current nuclear mass models and help better predict the masses as well as the neutron drip line ( $S_{2n} = 0$ ). Additionally, we can estimate the uncertainty in the neural networks by adding drop-out layers. The uncertainty tends to grow with extrapolation. Thus, the largest uncertainties in the drip line are in the trans-uranium ( $Z > 92$ ) region, where there is relatively few measurements and the extrapolation is largest.

Other nuclear mass model exist, and generally disagree once they are extrapolated beyond existing data. Using DJINN, each mass model could be refined and compared.

Other mass models to consider:  
 -FRDM  
 -HF3F-19, 21, 27  
 -MN  
 Other nuclear statistical parameters may also be predicted using BNN using similar methods.

## References

[1] R. Uliyan and J. Piekarewicz, Phys. Rev. C93, 044311 (2016)  
 [2] R. Uliyan and J. Piekarewicz, Phys. Rev. C96, 044338 (2017)  
 [3] K. D. Humbird et al., IEEE Trans. Nucl. Sci. 65(6), 1264-1275 (2018)  
 [4] K. Buium, Phys. Reports 621, 206 (2016)  
 [5] Y. Gai and Z. Ghoshanam, arXiv:1506.02142 (2016)

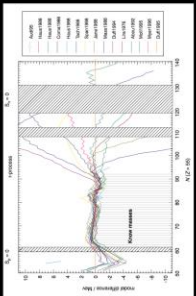
Using 2,407 experimentally measured masses from the 2016 Atomic Mass Adjustment (AME=2016) with  $Z_{\text{N}} > 8$ , DJINN is trained on the mass residuals

$$\text{Res}(Z, N) = M_{\text{AME}}(Z, N) - M_{\text{fit}}(Z, N)$$

Where  $M_{\text{fit}}$  is the model mass prediction. We chose to investigate the microscopic DoThe-Zucker 10 parameter model and the macroscopic Liquid Drop model using the same parameters in [2].

To test the neural network, it is trained on 80% of the data ( $\sim 1,800$  nuclei) and predicts the remaining 20% of data that has not yet seen (see table below).

A drop-out percentage of 5% is used as a Bayesian Approximation to quantify the uncertainties in the model.



The chart of nuclides with black squares stable isotopes observed in nature. The red curve is DJ-DJINN's prediction of the neutron drip line ( $S_{2n} = 0$ ) using the DJ model refined by DJINN. Due to the Drop-Out Bayesian Approximation, an uncertainty can be estimated which gives a thickness to the drip line, spanning several isotopes among certain  $Z$  chains (ev  $Z = 51$  Sh).

The BNN residual predictions are compared to the experimental values. A perfect agreement would lie on the dashed red line, which is a visual aid.



# Infrared Absorption Spectroscopy to Study Oxide Formation in Laser Produced Plasmas for Nuclear Forensics Applications

L. A. Finney\*, D. G. Weisz, B. Koroglu, and J. Crowhurst

## Lawrence Livermore National Laboratory

**Abstract:** Current models for nuclear fireball expansion and chemistry are outdated, and modern analytical techniques can help fill the gaps. One example is using laser ablation to produce high temperature, rapidly cooling, dynamic plasma plumes as a surrogate for a fireball. Both the material being ablated and surrounding environment conditions, such as air composition, significantly alter the chemistry that takes place. Here we explore the potential for infrared absorption spectroscopy of LPP chemistry to yield information about metal oxide formation.

### Nuclear fireballs undergo complex chemical reactions that are not well understood

Molten and vapor phase species in a fireball eventually cool to form particulates and solids of varying composition.

Trinitite sample



The figure<sup>2</sup> below shows how:

- Fine, overlapping atomic and ionic lines
- Broad oxide emissions are overshadowed

Laser produced plasmas (LPPs) can act as surrogate for nuclear explosions to study high temperature chemistry.

The figure<sup>3</sup> below shows how LPPs have rapidly changing temperature with time. The cooling timescales for a nuclear fireball is on the order of seconds.

Shadowgrams of laser produced plasmas from a solid Si target<sup>4</sup>. This shows the plasma expansion and shockwave expansion plume, similar to a high temperature metal expansion.

Shadowgrams of laser produced plasmas from a solid Si target<sup>4</sup>. This shows the plasma expansion and shockwave expansion plume, similar to a high temperature metal expansion.

Shadowgrams of laser produced plasmas from a solid Si target<sup>4</sup>. This shows the plasma expansion and shockwave expansion plume, similar to a high temperature metal expansion.

Shadowgrams of laser produced plasmas from a solid Si target<sup>4</sup>. This shows the plasma expansion and shockwave expansion plume, similar to a high temperature metal expansion.

Shadowgrams of laser produced plasmas from a solid Si target<sup>4</sup>. This shows the plasma expansion and shockwave expansion plume, similar to a high temperature metal expansion.

Shadowgrams of laser produced plasmas from a solid Si target<sup>4</sup>. This shows the plasma expansion and shockwave expansion plume, similar to a high temperature metal expansion.

Shadowgrams of laser produced plasmas from a solid Si target<sup>4</sup>. This shows the plasma expansion and shockwave expansion plume, similar to a high temperature metal expansion.

Shadowgrams of laser produced plasmas from a solid Si target<sup>4</sup>. This shows the plasma expansion and shockwave expansion plume, similar to a high temperature metal expansion.

Shadowgrams of laser produced plasmas from a solid Si target<sup>4</sup>. This shows the plasma expansion and shockwave expansion plume, similar to a high temperature metal expansion.

Shadowgrams of laser produced plasmas from a solid Si target<sup>4</sup>. This shows the plasma expansion and shockwave expansion plume, similar to a high temperature metal expansion.

Shadowgrams of laser produced plasmas from a solid Si target<sup>4</sup>. This shows the plasma expansion and shockwave expansion plume, similar to a high temperature metal expansion.

Shadowgrams of laser produced plasmas from a solid Si target<sup>4</sup>. This shows the plasma expansion and shockwave expansion plume, similar to a high temperature metal expansion.

Shadowgrams of laser produced plasmas from a solid Si target<sup>4</sup>. This shows the plasma expansion and shockwave expansion plume, similar to a high temperature metal expansion.

Shadowgrams of laser produced plasmas from a solid Si target<sup>4</sup>. This shows the plasma expansion and shockwave expansion plume, similar to a high temperature metal expansion.

Shadowgrams of laser produced plasmas from a solid Si target<sup>4</sup>. This shows the plasma expansion and shockwave expansion plume, similar to a high temperature metal expansion.

Shadowgrams of laser produced plasmas from a solid Si target<sup>4</sup>. This shows the plasma expansion and shockwave expansion plume, similar to a high temperature metal expansion.

Shadowgrams of laser produced plasmas from a solid Si target<sup>4</sup>. This shows the plasma expansion and shockwave expansion plume, similar to a high temperature metal expansion.

Shadowgrams of laser produced plasmas from a solid Si target<sup>4</sup>. This shows the plasma expansion and shockwave expansion plume, similar to a high temperature metal expansion.

Shadowgrams of laser produced plasmas from a solid Si target<sup>4</sup>. This shows the plasma expansion and shockwave expansion plume, similar to a high temperature metal expansion.

Shadowgrams of laser produced plasmas from a solid Si target<sup>4</sup>. This shows the plasma expansion and shockwave expansion plume, similar to a high temperature metal expansion.

Shadowgrams of laser produced plasmas from a solid Si target<sup>4</sup>. This shows the plasma expansion and shockwave expansion plume, similar to a high temperature metal expansion.

Shadowgrams of laser produced plasmas from a solid Si target<sup>4</sup>. This shows the plasma expansion and shockwave expansion plume, similar to a high temperature metal expansion.

Shadowgrams of laser produced plasmas from a solid Si target<sup>4</sup>. This shows the plasma expansion and shockwave expansion plume, similar to a high temperature metal expansion.

Shadowgrams of laser produced plasmas from a solid Si target<sup>4</sup>. This shows the plasma expansion and shockwave expansion plume, similar to a high temperature metal expansion.

Shadowgrams of laser produced plasmas from a solid Si target<sup>4</sup>. This shows the plasma expansion and shockwave expansion plume, similar to a high temperature metal expansion.

Shadowgrams of laser produced plasmas from a solid Si target<sup>4</sup>. This shows the plasma expansion and shockwave expansion plume, similar to a high temperature metal expansion.

Shadowgrams of laser produced plasmas from a solid Si target<sup>4</sup>. This shows the plasma expansion and shockwave expansion plume, similar to a high temperature metal expansion.

Shadowgrams of laser produced plasmas from a solid Si target<sup>4</sup>. This shows the plasma expansion and shockwave expansion plume, similar to a high temperature metal expansion.

Shadowgrams of laser produced plasmas from a solid Si target<sup>4</sup>. This shows the plasma expansion and shockwave expansion plume, similar to a high temperature metal expansion.

Shadowgrams of laser produced plasmas from a solid Si target<sup>4</sup>. This shows the plasma expansion and shockwave expansion plume, similar to a high temperature metal expansion.

Shadowgrams of laser produced plasmas from a solid Si target<sup>4</sup>. This shows the plasma expansion and shockwave expansion plume, similar to a high temperature metal expansion.

Shadowgrams of laser produced plasmas from a solid Si target<sup>4</sup>. This shows the plasma expansion and shockwave expansion plume, similar to a high temperature metal expansion.

Shadowgrams of laser produced plasmas from a solid Si target<sup>4</sup>. This shows the plasma expansion and shockwave expansion plume, similar to a high temperature metal expansion.

Shadowgrams of laser produced plasmas from a solid Si target<sup>4</sup>. This shows the plasma expansion and shockwave expansion plume, similar to a high temperature metal expansion.

Shadowgrams of laser produced plasmas from a solid Si target<sup>4</sup>. This shows the plasma expansion and shockwave expansion plume, similar to a high temperature metal expansion.

Shadowgrams of laser produced plasmas from a solid Si target<sup>4</sup>. This shows the plasma expansion and shockwave expansion plume, similar to a high temperature metal expansion.

Shadowgrams of laser produced plasmas from a solid Si target<sup>4</sup>. This shows the plasma expansion and shockwave expansion plume, similar to a high temperature metal expansion.

### High-Z element-oxides are challenging to observe with QES

This method can be challenging for high-Z elements like uranium.

The figure<sup>5</sup> below shows how:

- Fine, overlapping atomic and ionic lines

- Broad oxide emissions are overshadowed

QCL and Hennert cell arrangement allows for multiple passes through a sample

Trinitite sample

NaCl + sample

Hennert cell

QCL

Hennert cell + chamber

MCT

detector

Single pass

20 passes in Hennert cell

Single pass

multiple passes

Abundance

Wavenumbers (cm<sup>-1</sup>)

Increasing the number of passes through the chamber enhances the signal measured – improving probability for detecting species in small quantities.

### FTIR analysis confirms signal from QCL absorption of Al oxides

SEM and EDX images showing Al<sub>2</sub>O<sub>3</sub> particles deposited onto NaCl windows from laser ablation of Al in air

Wavenumbers (cm<sup>-1</sup>)

1.0

0.8

0.6

0.4

0.2

0.0

1.0

0.8

0.6

0.4

0.2

0.0

1.0

0.8

0.6

0.4

0.2

0.0

1.0

0.8

0.6

0.4

0.2

0.0

1.0

0.8

0.6

0.4

0.2

0.0

1.0

0.8

0.6

0.4

0.2

0.0

1.0

0.8

0.6

0.4

0.2

0.0

1.0

0.8

0.6

0.4

0.2

0.0

1.0

0.8

0.6

0.4

0.2

0.0

1.0

0.8

0.6

0.4

0.2

0.0

1.0

0.8

0.6

0.4

0.2

0.0

1.0

0.8

0.6

0.4

0.2

0.0

1.0

0.8

0.6

0.4

0.2

0.0

1.0

0.8

0.6

0.4

0.2

0.0

1.0

0.8

0.6

0.4

0.2

0.0

1.0

0.8

0.6

0.4

0.2

0.0

1.0

0.8

0.6

0.4

0.2

0.0

1.0

0.8

0.6

0.4

0.2

0.0

1.0

0.8

0.6

0.4

0.2

0.0

1.0

0.8

0.6

0.4

0.2

0.0

1.0

0.8

0.6

0.4

0.2

0.0

1.0

0.8

0.6

0.4

0.2

0.0

1.0

0.8

0.6

0.4

0.2

0.0

1.0

0.8

0.6

0.4

0.2

0.0

1.0

0.8

0.6

0.4

0.2

0.0

1.0

0.8

0.6

0.4

0.2

0.0

1.0

0.8

0.6

0.4

0.2

0.0

1.0

0.8

0.6

0.4

0.2

0.0

1.0

0.8

0.6

0.4

0.2

0.0

1.0

0.8

0.6

0.4

0.2



# Quantifying Uncertainty in Inter-Laboratory Thermal Calibration Exercise

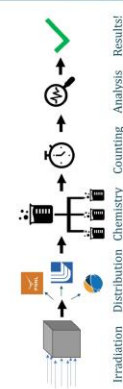
C. Apgar<sup>1</sup>, P. Zhao<sup>2</sup>

<sup>1</sup>University of California, Berkeley, Berkeley, CA 94701  
<sup>2</sup>Lawrence Livermore National Laboratory, Livermore, CA 94550

## Overview:

Nuclear forensics plays a vital role in protecting national security. A ratio-of-ratios, known as the R-value, is used in this exercise. This study seeks to identify the sources of uncertainty and introduce mitigating tools to reduce overall uncertainty and increase accuracy of results.

$$R_{\gamma} = \frac{\left( \frac{\text{Atoms of } {}^{99}\text{Mo}_{\text{exp}}}{\text{Atoms of } {}^{99}\text{Mo}_{\text{ref}}} \right)}{\left( \frac{\text{Cumulative Fission Yield } X}{\text{Cumulative Fission Yield } {}^{99}\text{Mo}} \right)}$$



## Method:

Analytical data for the exercise can be divided into 3 sections. Each of these sections was independently reviewed and collectively analyzed for sources and impact on uncertainty and accuracy.



Chemistry



Nuclear Counting Data



Nuclear Data

## Chemistry

### Chemistry Process:

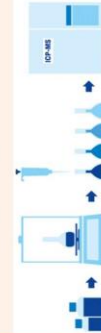
Potential errors associated with chemical processes, such as cross contamination, can be detected by reviewing standard deviation among separated samples. Results on Cerium samples, for example, showed that removing statistical outliers greatly improved R-value accuracy:

### Original sample results...

Isotope	$\sigma$	R-Value
141Ce	22%	0.69
143Ce	22%	0.65
144Ce	23%	0.75

### ICP-MS Yields:

Yield calculations introduced an uncertainty of between 0.1% and 2.9% to sample measurements. Dilution chemistry was calculated to introduce between .3% and 1.2% uncertainty to sample measurements.



## Nuclear Counting Data

### Detector Calibration:

R-values were calculated on a by-detector basis before being weighted in order to remove inherent detector uncertainty. In sample cases, this showed dramatic improvement in both reducing uncertainty and increasing accuracy.



### Gamma Energies and Intensities:

A review of gamma spectroscopy results was completed. While GAMANAL provided consistent results, further review of calculations is necessary to determine accuracy.



## Nuclear Data

### Decay Correction Factors:

Factors were updated to use the latest NNDC data, including uncertainty. Uncertainty ranged from .01% to .05%.

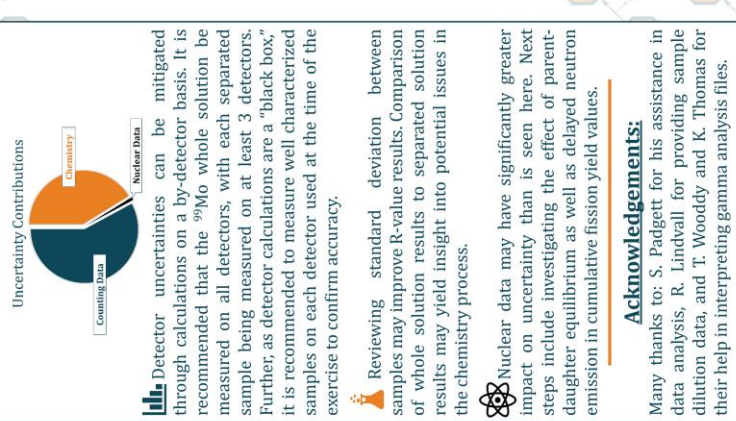
### Cumulative Fission Yields:

Uncertainties are unavailable for cumulative fission yields. However, by modeling target nuclide population during and after irradiation, it becomes apparent that certain nuclide fission yields may not be accurate for the irradiation period of this exercise, thus leading to inaccurate R-values.



This work performed under the auspices of the U.S. Department of Energy by Lawrence Livermore National Laboratory under Contract DE-AC52-07NA27344.

LLNL-POST-782919



## Acknowledgements:

Many thanks to: S. Padgett for his assistance in data analysis, R. Lindau for providing sample dilution data, and T. Woody and K. Thomas for their help in interpreting gamma analysis files.





# Enhancing Resonance Ionization Mass Spectrometry at LLNL: Automated sub-nanosecond timing control to maintain sensitivity and mass resolution

Jacob S. Lewis<sup>1,2</sup>, Brett Isselhardt<sup>3</sup>

<sup>1</sup>Nano-Device Laboratory (NDL) and Phonon Optimized Engineered Materials (POEM) Center  
<sup>2</sup>Materials Science and Engineering Program, University of California, Riverside  
<sup>3</sup>Lawrence Livermore National Lab

## Abstract

Resonance Ionization Mass Spectrometry (RIMS) offers unparalleled selectivity of species in the determination of isotopic mass from samples of diverse elemental constitution. Thus property of the technique emerges from the excitation at any given element's characteristic and narrow absorption band to promote a bound electron to a higher energy state. Successive excitations are applied at the appropriate energies such that only the intended elements are ionized and accelerated into a mass spectrometer. The work reported at present is concerned with the requisite tight timing constraints of ablation sources, successive ionization lasers, and signal detectors employed in this technique. A single, unifying graphical user interface software was developed for the control and automation of experimental elements. Improvement of the timings of these sources will serve to enhance the instrument's mass resolution, sensitivity, efficiency, reproducibility, and the operator's ease-of-use.

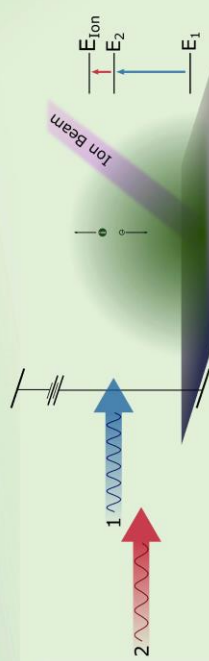
## Introduction

► The RIMS technique is dependent on the tight timing tolerances of experimental components. For instance, if the ion excitation lasers fire prior to or too late after the ion beam ablates the surface of the sample no signal will be detected.  
 ► Programmatic control of components will ensure reliable timings of the equipment.  
 ► Alone, this solution does not address the time evolution of the beam spectral center of gravity inherent in real-world laser systems.

► This will be addressed by continuous monitoring of the beams' spectral center of gravity and programmatically apply slight adjustments to the angle of the Ti:Sapphire lasers diffraction grating, thus creating an automatic control feedback loop.  
 ► The equipment used to control the RIMS components are SRS DG645 digital delay generators.  
 ► Automatic communication is established via SPI commands passed from computer by python 3.7 through ethernet networking.  
 ► A Graphical User Interface (GUI) was designed to provide a unifying control system.  
 ► Periodic monitoring of oscilloscope measurements of beam spectra and the adjustment of timings will address the undesired time evolution of the beams' spectral centers of gravity.

## Results

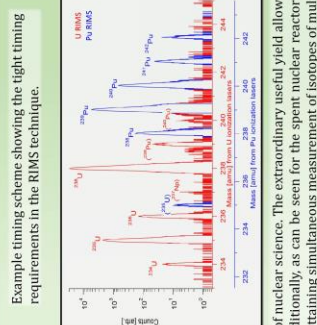
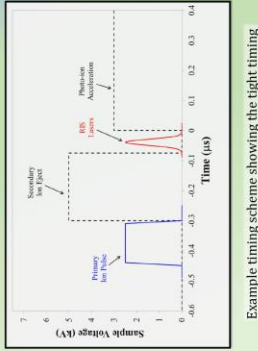
► Programmatic control of the instruments' components has been achieved in a single, unifying GUI.  
 ► The LION instrument's ease-of-use and speed of operation has been improved.  
 ► Still to be completed is the automatic monitoring and control of the lasers' spectral center of gravity.



Schematic figure of RIMS technique's interaction with samples. Initially, an ablation source such as an ion beam strikes the sample and spatters atoms of the sample. Then a series of laser pulses impinge upon the atom cloud to successively promote the electrons of the targeted element.



Picture of the LION system with lasers and optical elements to the left and the sample chamber and mass spectrometer on the right.



Example timing scheme showing the tight timing requirements in the RIMS technique.

## Discussion

► The success of the GUI has proven the viability of further automation of this niche technique and could prove to be a vital component in the push towards popularization of the method.  
 ► The future implementation of beam sampling and automatic control could prove an important step in the future full automation of the LION instrument at LLNL.



Screenshot of the simplified view screen of the control GUI developed in python 3.7 and PyQt5.



# Measuring Surface Roughness on $\text{UO}_2$ Fuel Pellets for Nuclear Forensics

Meena Said<sup>1</sup>, Charlotte W. Eng<sup>2</sup>, and Naomi E. Marks<sup>2</sup>

<sup>1</sup>University of Notre Dame, Notre Dame, IN 46556

<sup>2</sup>Lawrence Livermore National Laboratory, Livermore, Nuclear and Chemical Sciences Division

## INTRODUCTION

Information regarding the bulk composition, macroscopic properties, trace impurities, and isotopic composition of elements is crucial to assemble any practical conclusions from a given sample regarding production location and/or process history (Moody et al., 2014). The enrichment and fabrication of uranium into  $\text{UO}_2$  fuel pellets plays a major role within the nuclear fuel cycle.  $\text{UO}_2$  fuel pellets undergo grinding procedures to create their cylindrical shape with dimensions set by the production plant's specifications. Previous studies have shown that measuring  $\text{UO}_2$  fuel pellet surface roughness via profilometry can indicate production location based on the grinding method (Pajo et al., 2001). There is currently no standard procedure in place to measure surface roughness of  $\text{UO}_2$  fuel pellets and still little to suggest it could play a role as a robust forensic signature. This work aims to determine a best practices method for accurately measuring surface roughness to determine fuel pellet provenance.

## SAMPLE PREPARATION

Samples of interest for this method development study include:

- Natural fuel pellet, intact
- Fuel pellet piece, 3-4%  $^{235}\text{U}$  enrichment
- Fuel pellet piece, 17%  $^{235}\text{U}$  enrichment
- Images of each sample can be found in Figure 1, and physical measurements were acquired using digital calipers, as seen in Table 1.



Figure 1.  $\text{UO}_2$  fuel pellets.

## Zygo ZeGage Optical Profilometer

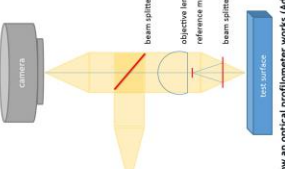


Figure 2. How an optical profilometer works (Adapted from Zygo).

## METHOD DEVELOPMENT

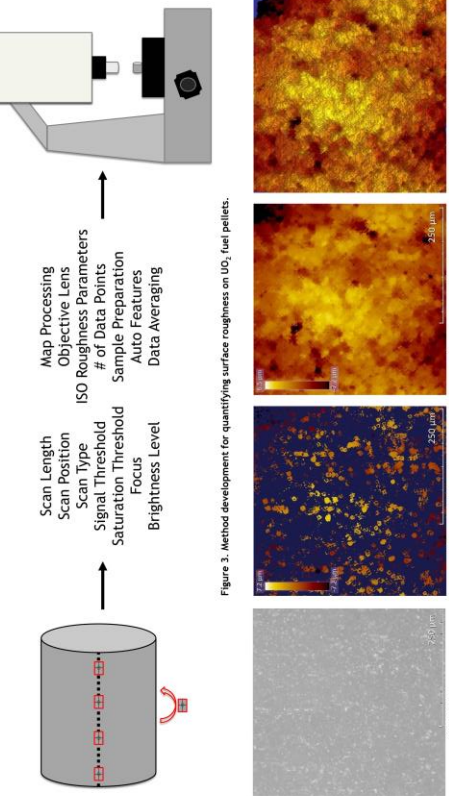


Figure 3. Method development for quantifying surface roughness on  $\text{UO}_2$  fuel pellets.

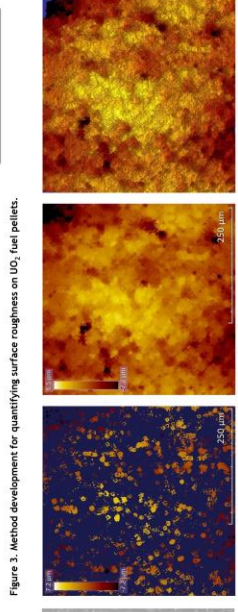


Figure 4. Data acquisition and map processing.

## RESULTS

Table 1. Diameters, average areal surface roughness ( $S_a$ ) and average profile surface roughness ( $R_a$ ) of  $\text{UO}_2$  fuel pellets.

Sample Name	Reactor Type	Diameter (mm)	Hole Diameter (mm)	Height (mm)	$S_a$ ( $\mu\text{m}$ )	Std Dev (σ)	$R_a$ ( $\mu\text{m}$ )	Std Dev (σ)
EC-NRH-106	1	10.62 ± 0.01	N/A	12.16 ± 0.01	1.68	0.11	1.39	0.17
CRM 125-A <sup>1</sup>	2	8.15 ± 0.08	N/A	9.96 ± 0.17	1.82	0.10	1.82	0.22
18-001 <sup>1</sup>	3	5.77 ± 0.02	1.71 ± 0.01	9.01 ± 0.01	2.90	0.34	2.90	0.48

<sup>1</sup>Physical measurements of intact pellets were taken from previous work.

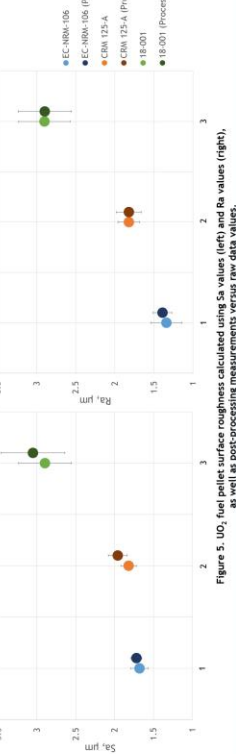


Figure 5.  $\text{UO}_2$  fuel pellet surface roughness calculated using  $S_a$  values (left) and  $R_a$  values (right), as well as post-processing measurements versus raw data values.

## DISCUSSION

Project Objectives:

- What parameters will be used to determine surface roughness of the material?
- How many analyses are necessary per sample to acquire a sufficient amount of surface roughness data?
- What are the differences between fuel pellets that have not undergone grinding versus fuel pellets that have?
- Is it possible to differentiate provenance through surface roughness measurements using optical profilometry?

Takeaways:

- The traditionally used  $R_a$  value for quantifying surface roughness via 2D profile measurements is variable and representative of a small sample set.
- $S_a$  values pertain to the roughness average of a 3D areal view of the surface, providing a more complete picture of the bulk while maintaining constrained uncertainties.
- Parameters such as scan length and measurements per sample were optimized for efficiency and accuracy.
- 5 regions along the length of the fuel pellet were measured, within a 400 × 400  $\mu\text{m}$  area.
- For shorter pellets, 5 regions along the cylinder were measured within a 400 × 400  $\mu\text{m}$  area.
- Fuel pellet fragment from producer 3, which showed signs of no grinding, displayed the highest surface roughness values.

## REFERENCES

Moody, M. J.; Grant, P.M.; Hutchison, I.D. Nuclear forensics: analysis; CRC Press: Boca Raton, FL, 2014.

Palo, L.; Schubert, F.; Zilberman, L.; Koch, L.; Balashov, Y.K.; Dolgov, Y.M.; Chernobay, N. Identification of plutonium nuclear fuel by impurities and physical parameters. *J. Radionucl. Nucl. Chem.* 2001, 250 (1), 79-84.

Many thanks to those that provided the fuel pellets used for analysis. Thank you to Charlotte Eng for her willingness to help in more than one way along with aid on the DS550 optical microscope. Last but not least, thank you to Naomi Marks for her mentorship and for being best.

This work performed under the auspices of the U.S. Department of Energy by Lawrence Livermore National Laboratory under Contract DE-AC52-07NA2434.



Figure 6. Ongoing fuel pellet measurements.

Lawrence Livermore National Laboratory, the University of Notre Dame, and the University of Michigan, through the LLNL Nuclear Science and Security Summer Internship Program, have been granted the use of the LLNL Computing and Data Science Division's computing and data storage resources for the duration of the program. The LLNL Computing and Data Science Division's computing and data storage resources are provided by the LLNL Computing and Data Science Division, the LLNL Data Science and Analytics Group, and the LLNL Data Science and Analytics Group.